Zitierweise: *Angew. Chem. Int. Ed.* **2022,** *61,* e202114953
Internationale Ausgabe: doi.org/10.1002/anie.202114953
Deutsche Ausgabe: doi.org/10.1002/ange.202114953

VIP **Heterogeneous Catalysis** **Very Important Paper**

Highly Enhanced Aromatics Selectivity by Coupling of Chloromethane and Carbon Monoxide over H-ZSM-5

Xudong Fang, Hongchao Liu, Zhiyang Chen, Zhaopeng Liu, Xiangnong Ding, Youming Ni, Wenliang Zhu,* and Zhongmin Liu**

Abstract: The transformation of methane into high value-added chemicals such as aromatics provides a more desired approach towards sustainable chemistry but remains a critical challenge due to the low selectivity of aromatics and poor stability. Herein, we first report a coupling reaction of CH_3Cl and CO (CCTA) based on methane conversion, which achieves extremely high aromatics selectivity (82.2 %) with the selectivity of BTX up to ca. 60 % over HZSM-5. The promoting effects have been demonstrated on other zeolites especially 10-membered rings (10 MR) zeolites. Multiple characterizations show that 2,3-dimethyl-2-cyclopentene-1-one (DMCPO) is generated from acetyl groups and olefins. Furthermore, isotopic labeling analysis confirms that CO is inserted into the DMCPO and aromatics rings. A new aromatization mechanism is proposed, including the formation of the above intermediates, which conspicuously weakens the hydrogen transfer reaction, leading to a considerable increase of aromatics selectivity and a dramatic drop in alkanes.

Introduction

Due to the depletion of crude oil and the rising demands for transportable fuels, developments on sustainable production technologies from non-petroleum carbon resources, e.g., natural gas, coal, and biomass, are receiving widespread attention. Various syngas-based technologies have been developed and commercialized successfully to date,[1] but aromatics manufacturing technologies have not been commercialized due to low selectivity and poor stability.[2] In this case, aromatic synthesis technologies based on methanol/syngas have been thoroughly researched and focused on modifying ZSM-5 zeolite.[2,3] Despite tremendous advances, aromatic selectivity and catalyst stability continue to be key problems. Consequently, exploiting an efficient approach for aromatic production from non-petroleum resources is critical for the sustainable chemical industry.

Natural gas has become a vital and alternative non-petroleum resource for aromatics production following the breakthrough of hydraulic fracturing technology.[4] Direct methane conversion with or without the assistance of small molecule compounds, e.g., oxygen,[5] CO,[6] and methanol,[7] appears to be more economical and environmentally friendly. However, the relatively highly inert nature of methane, resulting from the high C–H bond strength and supersymmetric structure, makes it challenging.[8] Moreover, the indirect pathway via syngas/methanol is still in the laboratory-scale stage.[2] In doing so, despite significant attempts to overcome the problem of low aromatics selectivity and fast deactivation of catalysts during methane conversion,[9] the slow progress has impeded the further development of methane to aromatics.

Methyl halide, a vital platform chemical for the transformation of methane, can be obtained readily from methane halogenation under moderate reaction conditions with high yields,[10] and also easily converted to high value-added chemicals and liquid fuels.[11] Studies on methyl halide to olefins, in particular, were carried out over SAPO-34 at 723 K, 0.1 MPa, obtaining up to 95 % ethylene and propylene selectivity.[11,12] However, few investigations on the synthesis of aromatics by methyl halide have been published, with the majority of them focusing on CH_3Br-to-aromatics over HZSM-5[13] or modified ZSM-5 zeolites.[14] It is apparent that under the conditions of <673 K and 0.1 MPa, 100 % conversion of CH_3Br was achieved. Unfortunately, the selectivity to aromatics is not high (<50 %) in all reports owing to the inevitable formation of alkanes via a hydrogen transfer reaction caused by the difference in the H/C ratios between methyl halide and aromatics, particularly for BTX.[2] Thus, development of a novel route for the conversion of CH_3Cl to aromatics with high catalytic performance is attractive, while there remains significant challenges.

Herein, we present an effective strategy for the selective conversion of CH_3Cl to aromatics, especially BTX, by CH_3Cl carbonylation over H-zeolites with 10 MR. Up to 82.2 % aromatics selectivity with ca. 60 % BTX was obtained along with the complete conversion of CH_3Cl over HZSM-5 at 673 K and 5.0 MPa. The insertion of CO weakens the occurrence of the hydrogen transfer reaction, resulting in a significant increase of aromatics selectivity. Furthermore,

[*] X. Fang, Dr. H. Liu, Dr. Z. Chen, Z. Liu, X. Ding, Dr. Y. Ni, Prof. Dr. W. Zhu, Prof. Dr. Z. Liu
National Engineering Laboratory for Methanol to Olefins, Dalian Institute of Chemical Physics, Chinese Academy of Sciences
Dalian 116023 (P. R. China)
E-mail: chliu@dicp.ac.cn
wlzhu@dicp.ac.cn
liuzm@dicp.ac.cn
X. Fang, Dr. Z. Chen, Z. Liu, X. Ding
University of Chinese Academy of Sciences
Beijing 100049 (China)

DMCPO is proven to be synthesized from acetyl groups and olefins. This work contributes to broadening approaches towards the transformation of methane into chemicals in a sustainable way.

Results and Discussion

ZSM-5, an efficient catalyst for the production of aromatics from oxygenates and hydrocarbons, is first employed as a catalyst for the coupling of CH_3Cl and CO. Figure 1a shows that the product distribution changes significantly after introducing CO instead of N_2 under reaction conditions of 0.1 MPa, 673 K, and 3000 mL g_{cat}^{-1} h^{-1}. Remarkably, the selectivity of aromatics increases from 11.6 to 40.5 % at ambient pressure, whereas C_2–C_4 olefins selectivity dramatically decreases from 68.5 to 36.7 %. The corresponding aromatic selectivity varies from 1.4 to 5.9 % for toluene, 2.6 to 11.6 % for xylene, 3.3 to 14.7 % for A9 and 1.6 to 4.2 % for A10 in the products after the introduction of CO instead of N_2 (Figure S1). It is worth noting that about 7 % of oxygenates, including acetone, acetic acid, and methyl acetate, were detected in the products after introducing CO. These findings differ from the results based on the hydrogen transfer mechanism such as methanol/alkanes-to-aromatics,[2,15] indicating that a significant change in the reaction networks may occur during the CH_3Cl conversion to aromatics in the presence of CO.

As demonstrated in Figure 1b, the reaction pressure is an important factor in converting CH_3Cl to aromatics, and a higher reaction pressure promotes the formation of aromatics in the presence of CO. In comparison to the ambient data, the aromatics selectivity increases to 71.2 % at 1.0 MPa with complete conversion of CH_3Cl. More surprisingly, aromatics selectivity as high as 82.2 % (BTX selectivity up to 59.3 %) is obtained at the reaction pressure of 5.0 MPa, which is far higher than any prior results reported in the literature.[14] Simultaneously, the oxygenates existing at ambient pressure vanish completely, and the selectivity to $C_2^=$–$C_4^=$ is low to about 2.1 % in the products. It should be noted that the selectivity to methane and C_2–C_4 gaseous hydrocarbons decrease with increasing selectivity to aromatics, indicating that the hydrogen transfer reaction is

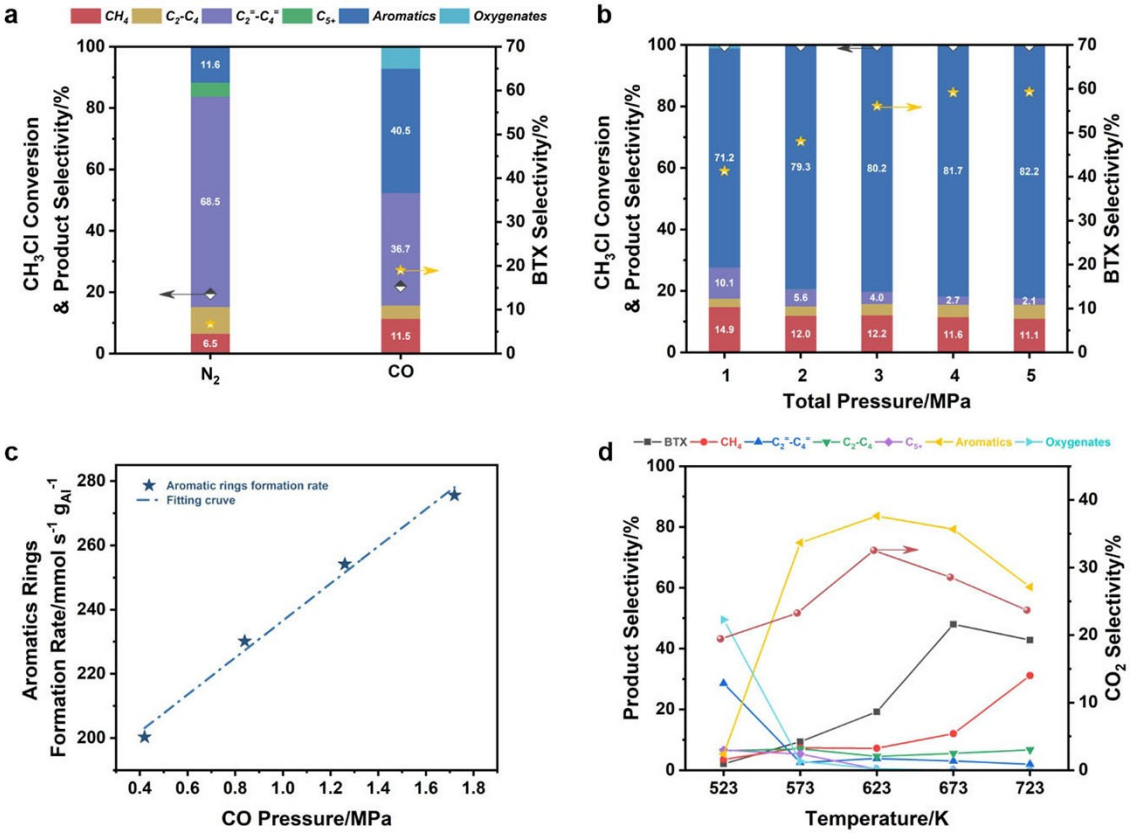

Figure 1. Catalytic performance of ZSM-5 with CO co-feeding at sub-complete chloromethane conversion. a) Catalytic performance in chloromethane-to-aromatics under N_2 and CO co-feeding. b) Catalytic performance in the CCTA reaction under different total pressures. c) The aromatics rings formation rate with different CO partial pressures. d) Catalytic performance in CCTA reaction at different reaction temperatures. Reaction conditions: a) 673 K, $P(N_2$ or CO) = 86 kPa, $P(CH_3Cl)$ = 0.7 kPa, Ar as balance gas, 0.1 MPa, 3000 mL g_{cat}^{-1} h^{-1}; b) 673 K, 3000 mL g_{cat}^{-1} h^{-1}, Ar as balance gas. c) 673 K, 2.0 MPa, $P(CO)$ = 0.4–1.72 MPa, $P(CH_3Cl)$ = 0.014 MPa, Ar as balance gas, 3000 mL g_{cat}^{-1} h^{-1}; d) 2.0 MPa, $P(CO)$ = 1.72 MPa, $P(CH_3Cl)$ = 0.014 MPa, Ar as balance gas, 3000 mL g_{cat}^{-1} h^{-1}; C_2–C_4 represents paraffin, $C_2^=$–$C_4^=$ represents olefins, C_{5+} excludes aromatics, oxygenates include acetic acid, methyl acetate and acetone.

obviously suppressed with increasing the total pressure from 1.0 to 5.0 MPa.

Figure 1c depicts the change on aromatic formation rate with CO pressure during CH_3Cl conversion. The rate of aromatics rings formation increases monotonically with increasing CO partial pressure, implying that the formation of aromatics is closely related to CO similar with the coupling of small molecule compounds and CO.[3d,16] In addition, the trends in selectivity to C_2–C_4 alkanes (from 22.2 to 3.1 %) and olefins (from 23.6 to 5.6 %) are opposite to that of aromatics (from 39.0 to 79.3 %) with increasing partial pressure of CO (Figure S2). As a result, we further corroborate the significance of CO in enhancing aromatics selectivity. These results obtained with $HZSM_{145}$ zeolite at temperatures of 523–723 K and 2.0 MPa ($P(CO)$ = 1.72 MPa) are shown in Figure 1d and Figure S3. Note that a carbon balance of 96.2 % was obtained under reaction conditions of 2.0 MPa, 673 K, and 3000 mL g_{cat}^{-1} h^{-1} after 3 h. The selectivity to aromatics first increases with reaction temperature and then reaches the maximum of 82 % at 623 K. After that, the selectivity of aromatics declines with reaction temperature up to 723 K. However, the maximum selectivity to BTX is approximately 50 % at 673 K, followed by a slight decrease with temperature. It should be noted that, at the relatively low reaction temperature of 523 K, the majority of the products are oxygenates (up to about 49 %) and $C_2^=$–$C_4^=$ (about 30 %) with a few aromatics (around 3 %). Surprisingly, when the reaction temperature is raised from 523 to 573 K, most oxygenates and $C_2^=$–$C_4^=$ convert to aromatics. Therefore, we deduce that olefins and oxygenates are the critical intermediate compounds during the conversion of CH_3Cl to aromatics. The emergence of considerable oxygenates in CCTA, including methyl acetate, acetic acid, and acetone, might be attributed to carbonylation reactions of CH_3Cl with CO on zeolite. These imply that the presence of CO significantly inhibits the hydrogen-transfer reactions. On the other hand, properly increasing the temperature is beneficial to enhance the conversion of CH_3Cl (Figure S3) and CO (Figure S4), which fits with the thermodynamic analysis results that the Gibbs energy decreases with increasing reaction temperature (Figure S5). Remarkably, the $NZSM\text{-}5_{41}$ displays no obvious deactivation during the 100 h test (Figure S6), which the selectivity of aromatics and BTX maintain at ca. 80 % and ca. 50 %, respectively, with complete conversion of CH_3Cl.

Other than ZSM-5, typical zeolites such as MCM-22, ZSM-22, ZSM-35, MOR, BETA, Y, and SAPO-34 are employed in the CCTA reaction. The detailed textural properties and chemical characteristics of the zeolite samples are shown in Figures S7–S10, and Table S1. As shown in Figure 2a and Figure S11, different zeolites exhibit different promoting effects and product distribution in the CCTA reaction. Apparently, coupling conversion of CH_3Cl with CO favors the formation of aromatics on the zeolite catalyst with various topologies. Interestingly, the selectivity of aromatics markedly increases by 40.5 %, 41.8 %, and 56.0 % over ZSM-5, ZSM-22, and MCM-22, respectively (Figure 2a), outperforming other zeolites containing 8 MR or 12 MR. In particular, MCM-22, an aluminosilicate material with MWW framework type, exhibits a significant increase on aromatics selectivity (≈20×) in the presence of CO, while the low C_2–C_4 paraffin selectivity decreases (73.9 to 6.9 %). ZSM-22 with TON framework type also displays significantly enhanced aromatics selectivity (18.2 to 59.9 %) with CO. Nevertheless, only 25.5 % aromatics selectivity is obtained with 32.8 % olefins, and 13.0 % oxygenates in the products over ZSM-35 consisted of 8 MR and 10 MR (Figure S11). Low aromatics selectivity over ZSM-35 might be due to the low conversion of the intermediate formed in CCTA. In brief, our findings clearly demonstrate the applicability of our strategy of co-feeding CO to promote aromatics selectivity during CH_3Cl conversion over various zeolites especially with 10 MR.

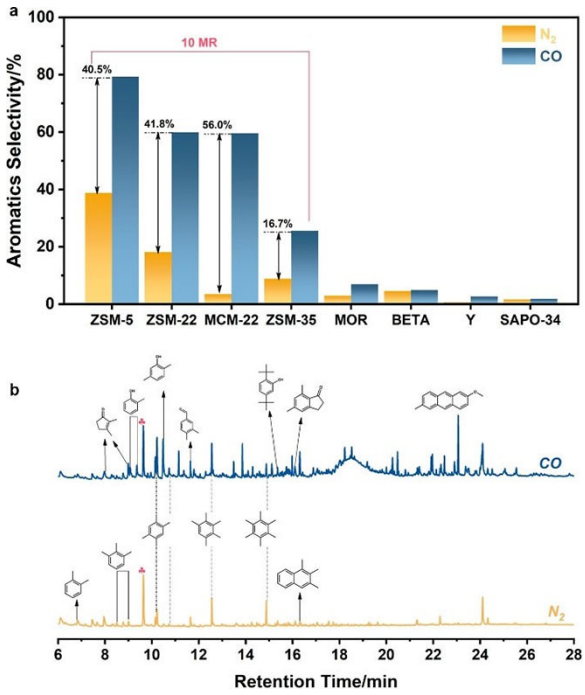

Figure 2. Catalytic performance over zeolites with different topologies. a) Aromatics selectivity in CCTA reaction under N_2 or CO co-feeding. b) GC-MS chromatograms of carbonaceous species retained in spent $HZSM\text{-}5_{145}$. Reaction conditions: 673 K, 2.0 MPa, P(CO or N_2) = 1.72 MPa, $P(CH_3Cl)$ = 0.014 MPa, Ar as balance gas, 3000 mL g_{cat}^{-1} h^{-1}.

In contrast to the hydrogen transfer mechanism in CH_3Br-to-aromatics[13,14] that a tremendous amount of light alkane formed during the CH_3Br conversion, the higher aromatics selectivity obtained in the current work is invariably accompanied by lower alkane selectivity over different 10 MR zeolites. Furthermore, oxygenates such as DMCPO extracted from spent zeolites after coupling conversion of CH_3Cl with CO are detected. Nevertheless, as seen in Figure 2b, the carbonaceous species are mainly polymethylbenzene with N_2 co-feeding, which is consistent with the hydrogen transfer mechanism. These results validate that there might exist another route of aromatics formation. Thus, it should be emphasized again that there

must exist another reaction mechanism for the CCTA reaction.

The study on the effect of contact time on product distribution can effectively explore the reaction intermediates, and the results are illustrated in Figure 3a. With decreasing contact time, the selectivity to olefins and oxygenates including acetic acid, methyl acetate and acetone increase gradually, whereas aromatics selectivity decreases. These findings suggest that the enhancement of aromatics formation should stem from the transformation of olefins and oxygenates initially generated in CCTA. Moreover, the selectivity of olefins and oxygenates obtained at 0.1 MPa are higher than that at 2.0 MPa regardless of whether the reactions are performed at 523 K or 673 K (Figure 1a, Figure 3b and Table S2). Increasing temperature under the same pressure, the aromatics selectivity significantly increases while the selectivity of olefins and oxygenates decreases which further confirms that aromatics might be produced from olefins and oxygenates. As a consequence, we preliminarily speculate that the observed improvements in aromatics selectivity result from the change of reaction mechanism under CO co-feeding, which olefins and oxygenates might form aromatics.

In order to further clarify the reaction mechanism, more experiments were conducted, including in situ DRIFT and ^{13}C isotope-labeling experiments. As shown in Figure 4a, the surface species over ZMS-5 are detected at different reaction temperatures. The negative peak at 3602 cm^{-1} is caused by the chemical adsorption of CH_3Cl. A wide peak appears at 3210 cm^{-1} below 523 K due to the physical adsorption of CH_3Cl[17] and gradually disappears with increasing temperature. Meanwhile, the new peaks at 2863 cm^{-1}, 2921 cm^{-1}, 2944 cm^{-1}, 2958 cm^{-1} and 2977 cm^{-1}, which are assigned to methoxy groups formed by the dissociation of CH_3Cl,[17] are observed to decrease as the temperature increases. These imply that CH_3Cl is initially adsorbed on Brønsted acid sites to form methoxy groups. Note that the peak at 1710 cm^{-1} attributed to acetyl groups[18] exists below 523 K but is difficult to detect at high temperature. Another new band at 1510 cm^{-1} appears at 573 K assigned to alkenyl carbonium ions in DMCPO[19] and gradually disappears as the temperature rises. These observations illustrate that the acetyl groups formed during the CCTA conversion to DMCPO and subsequently to aromatics sequentially. In addition, the reactions are stopped using liquid nitrogen, and the carbonaceous species confined in HZSM-5_{145} were analyzed (Figure 4b). Considerable DMCPOs are detected at 573 K and gradually decrease with increasing temperature, consistent with the change of peaks at 1710 cm^{-1} and 1510 cm^{-1}. The amount of polymethylbenzene increases with increasing temperature below 573 K and gradually decreases above 573 K because high temperature is conducive to the formation and desorption of aromatics. According to the above results, it is deduced that DMCPO is a crucial intermediate in the formation of aromatics generated from olefins and acetyl groups.

To validate our hypothesis, Figure 4c and d show the ^{13}C distribution in aromatics, propane, and propylene collected from the reaction of CH_3Cl and ^{13}CO. Figures S12–S14 provide a comprehensive analysis of the MS spectra of the product in the presence of ^{12}CO or ^{13}CO. Almost all aromatics contain at least one ^{13}C atom and the quantity of ^{13}C in aromatics is significantly higher than that in propylene, as shown in Figures 4c and d. As we know, the ^{13}C distribution in aromatics and olefins should be consistent if the aromatics are formed via the hydrogen transfer reaction. However, one ^{13}C atom in the product is mainly observed in our current work. Additionally, if aromatics are formed directly from oxygenates such as acetone and acetic acid, the product should mainly contain two or three ^{13}C atoms according to previous reports.[6,20] Therefore, these results reveal that CO participates in aromatics formation but follows a distinct mechanism. Moreover, the ^{13}C NMR spectra of the products exhibit some signal at 125–137 ppm attributed to the C atom at aromatic rings (Figure 4e), confirming that CO inserts into the aromatic rings and changes the reaction mechanism. To further understand the new reaction mechanism, we detected the active species

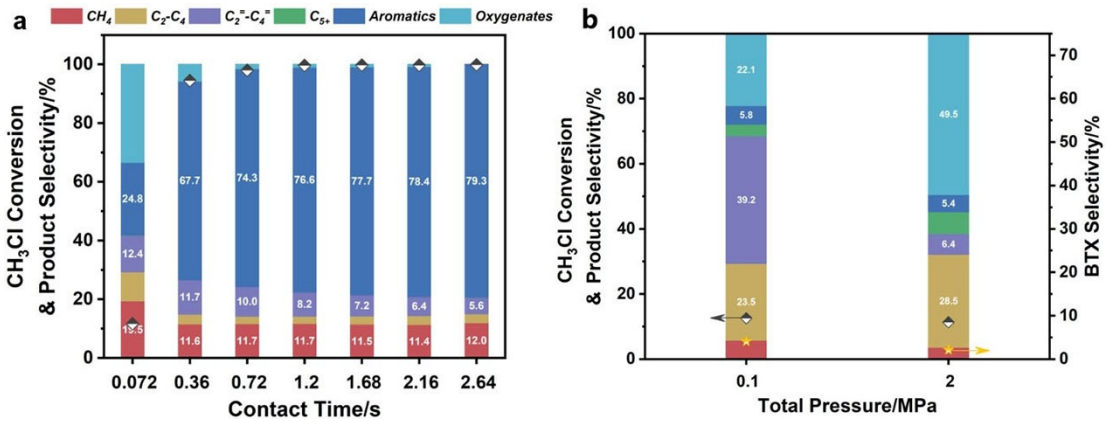

Figure 3. Catalytic performance over zeolites under different conditions in CCTA. a) Catalytic performance over HZSM-5_{145} at different contact times. b) Catalytic performance over HZSM-5_{145} under different total pressures. Reaction conditions: a) 673 K, 2.0 MPa, $P(CO) = 1.72$ MPa, $P(CH_3Cl) = 0.014$ MPa, Ar as balance gas; b) 523 K, 3000 mL g_{cat}^{-1} h^{-1}, $P(CO) = 1.72$ MPa, $P(CH_3Cl) = 0.014$ MPa, Ar as balance gas; Note that C_2–C_4 represents paraffin, $C_2^=$–$C_4^=$ represents olefins, C_{5+} excludes aromatics, oxygenates include acetic acid, methyl acetate and acetone.

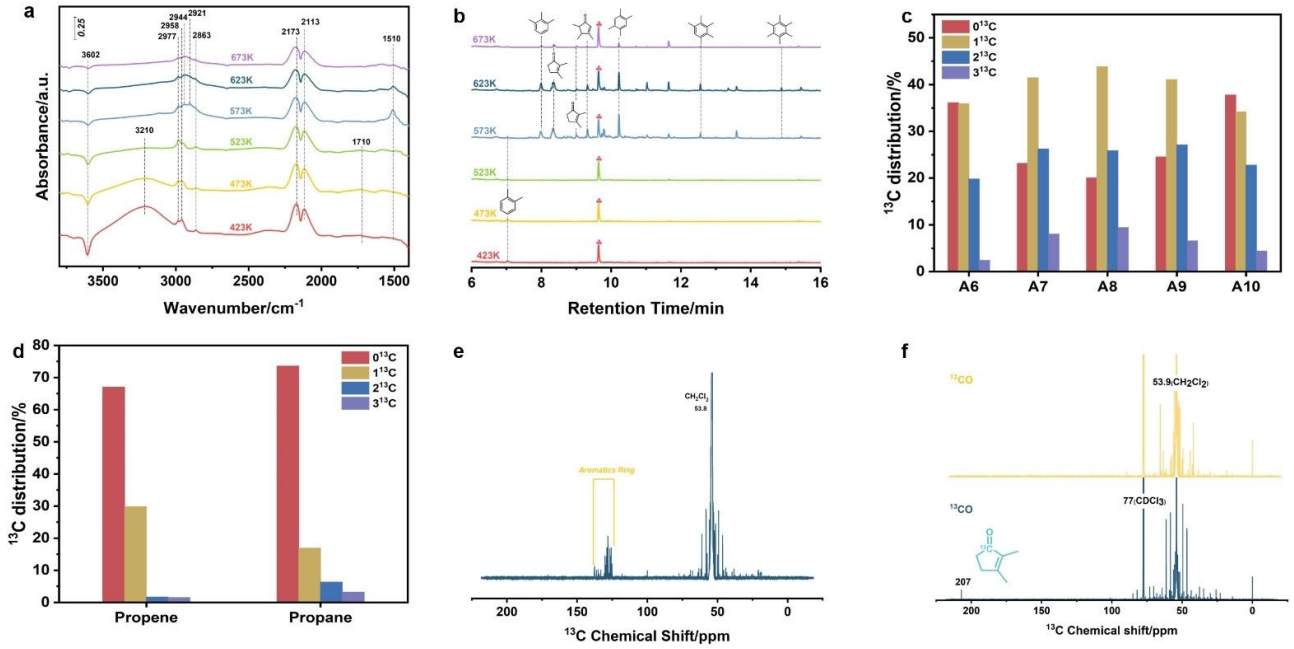

Figure 4. Characterization of the reaction mechanism. a) In situ DRIFT spectra from CCTA over ZSM-5_{36} with increasing reaction temperature. b) GC-MS chromatograms of organic materials retained in catalysis for different reaction temperatures collected from in situ DRIFT by liquid N_2. c) ^{13}C distribution in liquid products of the coupling reaction of CH_3Cl and ^{13}CO. d) ^{13}C distribution in propylene and propane collected from the coupling reaction of CH_3Cl. e) ^{13}C liquid-state NMR spectra of products in the presence of ^{13}CO during the CH_3Cl-to-aromatics reaction over HZSM-5_{145}. f) ^{13}C liquid-state NMR spectra of coke species in the presence of ^{13}CO during the CCTA reaction over ZSM-5_{145}. Reaction conditions: a) 1.0 MPa, 0.14 $g_{CH_3Cl}\, g_{cat}^{-1}\, h^{-1}$, $CO/CH_3Cl = 17$, Ar as balance gas; b c and d) HZSM-5_{145}, 673 K, 3150 mL $g_{cat}^{-1}\, h^{-1}$, $CO/CH_3Cl = 60$, Ar as balance gas, 1.0 MPa.

after quenching the reaction by liquid nitrogen by GC-MS. DMCPO is directly observed by GC-MS, which is considered an essential intermediate for aromatics formation (Figure S15). The ion fragments of the DMCPO detected by GC-MS display that ^{13}CO is incorporated into DMCPO, consistent with the ^{13}C distribution of products (Figure S16). Ulteriorly, the signal at 207 ppm collected by ^{13}C liquid-state NMR is attributed to the C atom in C=O, whereas other signals assigned to DMCPO cannot be observed (Figure 4f). The evidence clearly demonstrates that CO is incorporated into DMCPO and further converted into aromatics rings in the coupling of CH_3Cl and CO.

Overall, the enhancement of aromatics selectivity is mainly due to a shift in reaction mechanism, and the coupling reaction between olefins and oxygenates occurs more readily than olefins polymerization for the production of aromatics. Consequently, the reaction mechanism is proposed based on understanding the coupling of CH_3Cl and CO (Figure 5). 1) CH_3Cl is adsorbed on Si(OH)Al forming a methoxy and HCl. 2) The acetyl groups are generated from CO incorporated into methoxy groups. 3) The acetyl groups react with olefins such as propylene to form DMCPO. 4) These DMCPO further convert into aromatics after dehydration through a series of reactions.[21] Note that the carbonyl compounds, such as acetone and acetic acid, can also be converted to aromatics, as shown in Figure S17, which is consistent with the previous reports.[22] Meanwhile, the hydrogen transfer route might also be competitive with the new aromatization route. These mean

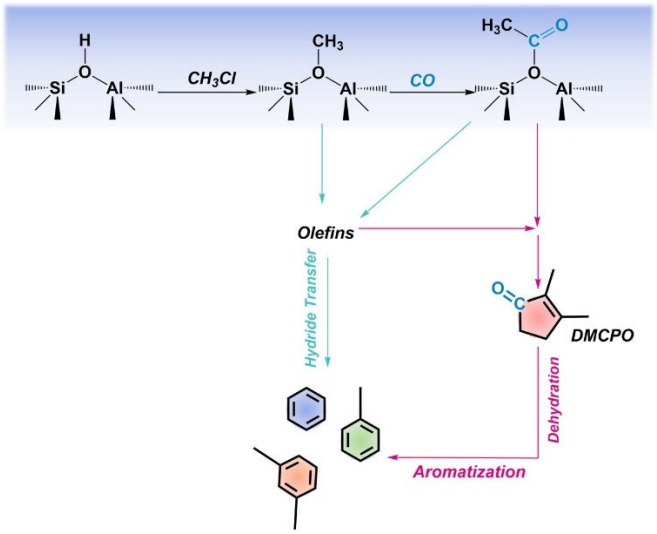

Figure 5. The proposed mechanism in the CCTA reaction over HZSM-5.

that the reaction network is complex in CCTA and indepth investigations are needed in the future.

Conclusion

In conclusion, we have proposed and demonstrated an enhanced aromatics production strategy enabled by coupling

CO with CH_3Cl over zeolites, especially with 10 MR. After introducing CO into CH_3Cl, the product distribution undergoes striking changes. Higher aromatics selectivity can be achieved along with fading of C_2–C_4 olefins and oxygenates by increasing the reaction pressure, CO partial pressure, and reaction temperature over HZSM-5. Under the conditions of 673 K, 5.0 MPa, and 3000 mL $g_{cat}^{-1} h^{-1}$, 82.2 % aromatics and ca. 60 % BTX selectivity are obtained, which are nearly 5-fold greater than those in the traditional conversion of CH_3Cl. Combined with in situ DRIFT and ^{13}C isotope-labeling experiments, CO has been proved to insert into aromatics in CCTA reactions leading to the improvement of aromatics selectivity. Furthermore, DMCPO is proved to be a significant intermediate generated from acetyl groups and olefins. Based on these results, a new aromatization for CH_3Cl-to-aromatics is proposed, in which the hydrogen transfer reaction is drastically suppressed. Altogether, this strategy offers a new idea for producing aromatics from non-petroleum resources and shows great potential for sustainable chemical industries.

Acknowledgements

We sincerely acknowledge the financial support from the National Natural Science Foundation of China (Grant No. 21972141, Grant No. 21991094 and Grant No. 21991090), the "Transformational Technologies for Clean Energy and Demonstration", the Strategic Priority Research Program of the Chinese Academy of Sciences (Grant No. XDA21030100), the Dalian High Level Talent Innovation Support Program (2017RD07), and the National Special Support Program for High Level Talents (SQ2019RA2TST0016). The authors thank Xiujuan Chi at the Dalian Institute of Chemical Physics, Chinese Academy of Sciences for the help with NMR measurements.

Conflict of Interest

The authors declare no conflict of interest.

Data Availability Statement

The data that support the findings of this study are available from the corresponding author upon reasonable request.

Keywords: Aromatics · Carbon Monoxide · Chloromethane · HZSM-5 · Methane Conversion

[1] a) K. Cheng, W. Zhou, J. Kang, S. He, S. Shi, Q. Zhang, Y. Pan, W. Wen, Y. Wang, *Chem* **2017**, *3*, 334–347; b) S. Kasipandi, J. W. Bae, *Adv. Mater.* **2019**, *31*, 1803390; c) A. Y. Khodakov, W. Chu, P. Fongarland, *Chem. Rev.* **2007**, *107*, 1692–1744; d) H. Xiong, L. L. Jewell, N. J. Coville, *ACS Catal.* **2015**, *5*, 2640–2658.

[2] T. Li, T. Shoinkhorova, J. Gascon, J. Ruiz-Martínez, *ACS Catal.* **2021**, *11*, 7780–7819.

[3] a) Y. Ni, W. Zhu, Z. Liu, *J. Energy Chem.* **2021**, *54*, 174–178; b) T. Shoinkhorova, T. Cordero-Lanzac, A. Ramirez, S.-h. Chung, A. Dokania, J. Ruiz-Martinez, J. Gascon, *ACS Catal.* **2021**, *11*, 3602–3613; c) P. Gao, J. Xu, G. Qi, C. Wang, Q. Wang, Y. Zhao, Y. Zhang, N. Feng, X. Zhao, J. Li, F. Deng, *ACS Catal.* **2018**, *8*, 9809–9820; d) Z. Chen, Y. Ni, Y. Zhi, F. Wen, Z. Zhou, Y. Wei, W. Zhu, Z. Liu, *Angew. Chem. Int. Ed.* **2018**, *57*, 12549–12553; *Angew. Chem.* **2018**, *130*, 12729–12733.

[4] a) Y. Tang, Y. Li, V. Fung, D. E. Jiang, W. Huang, S. Zhang, Y. Iwasawa, T. Sakata, L. Nguyen, X. Zhang, A. I. Frenkel, F. F. Tao, *Nat. Commun.* **2018**, *9*, 1231; b) Z. Jin, L. Wang, E. Zuidema, K. Mondal, M. Zhang, J. Zhang, C. T. Wang, X. J. Meng, H. Q. Yang, C. Mesters, F. S. Xiao, *Science* **2020**, *367*, 193–197.

[5] D. Li, W. S. Baslyman, B. Siritanaratkul, T. Shinagawa, S. M. Sarathy, K. Takanabe, *Ind. Eng. Chem. Res.* **2019**, *58*, 22884–22892.

[6] F. Wen, J. Zhang, Z. Chen, Z. Zhou, H. Liu, W. Zhu, Z. Liu, *Catal. Sci. Technol.* **2021**, *11*, 1358–1364.

[7] Y. Liu, D. Li, T. Wang, Y. Liu, T. Xu, Y. Zhang, *ACS Catal.* **2016**, *6*, 5366–5370.

[8] a) X. Li, C. Pei, J. Gong, *Chem* **2021**, *7*, 1755–1801; b) Y. Liu, D. Deng, X. Bao, *Chem* **2020**, *6*, 2497–2514; c) P. Schwach, X. Pan, X. Bao, *Chem. Rev.* **2017**, *117*, 8497–8520; d) P. Tang, Q. Zhu, Z. Wu, D. Ma, *Energy Environ. Sci.* **2014**, *7*, 2580–2591.

[9] a) N. Kosinov, E. J. M. Hensen, *Adv. Mater.* **2020**, *32*, 14; b) N. Kosinov, F. J. Coumans, E. Uslamin, F. Kapteijn, E. J. Hensen, *Angew. Chem. Int. Ed.* **2016**, *55*, 15086–15090; *Angew. Chem.* **2016**, *128*, 15310–15314.

[10] M. Bilke, P. Losch, O. Vozniuk, A. Bodach, F. Schuth, *J. Am. Chem. Soc.* **2019**, *141*, 11212–11218.

[11] R. Lin, A. P. Amrute, J. Perez-Ramirez, *Chem. Rev.* **2017**, *117*, 4182–4247.

[12] a) P. Wang, L. Chen, J.-K. Guo, S. Shen, C.-T. Au, S.-F. Yin, *Ind. Eng. Chem. Res.* **2019**, *58*, 18582–18589; b) D. Zhang, Y. wei, L. Xu, A. Du, F. Chang, B.-l. Su, Z. Liu, *Catal. Lett.* **2006**, *109*, 97–101.

[13] L. Tao, G.-S. Li, S.-F. Yin, Q. Ou-Yang, S.-L. Luo, X.-P. Zhou, C.-T. Au, *React. Kinet. Mech. Catal.* **2011**, *103*, 191–207.

[14] a) L. Tao, L. Chen, S.-F. Yin, S.-L. Luo, Y.-Q. Ren, W.-S. Li, X.-P. Zhou, C.-T. Au, *Appl. Catal. A* **2009**, *367*, 99–107; b) P. Wang, L. Chen, J. Xie, H. Li, C.-T. Au, S.-F. Yin, *Catal. Sci. Technol.* **2017**, *7*, 2559–2565; c) H. Chen, T. Chen, K. Chen, J. Fu, X. Lu, P. Ouyang, *Catal. Commun.* **2018**, *103*, 38–41.

[15] P. Del Campo, C. Martinez, A. Corma, *Chem. Soc. Rev.* **2021**, *50*, 8511–8595.

[16] C. Wei, Q. Yu, J. Li, Z. Liu, *ACS Catal.* **2020**, *10*, 4171–4180.

[17] Y. X. Wei, D. Z. Zhang, Z. M. Liu, B. L. Su, *J. Catal.* **2006**, *238*, 46–57.

[18] Z. Zhou, H. Liu, Y. Ni, F. Wen, Z. Chen, W. Zhu, Z. Liu, *J. Catal.* **2021**, *396*, 360–373.

[19] S. Kotrel, M. P. Rosynek, J. H. Lunsford, *J. Catal.* **2000**, *191*, 55–61.

[20] T. Yan, L. Yang, W. Dai, G. Wu, N. Guan, M. Hunger, L. Li, *ACS Catal.* **2019**, *9*, 9726–9738.

[21] a) Z. Liu, X. Dong, X. Liu, Y. Han, *Catal. Sci. Technol.* **2016**, *6*, 8157–8165; b) M. Hu, C. Wang, X. Gao, Y. Chu, G. Qi, Q. Wang, G. Xu, J. Xu, F. Deng, *ACS Catal.* **2020**, *10*, 4299–4305.

[22] a) Z. Cheng, S. Huang, Y. Li, K. Cai, Y. Wang, M.-y. Wang, J. Lv, X. Ma, *ACS Catal.* **2021**, *11*, 5647–5657; b) Z. Zhou, H. Liu, Z. Chen, W. Zhu, Z. Liu, *ACS Catal.* **2021**, *11*, 4077–4083.

Manuscript received: November 4, 2021
Accepted manuscript online: February 1, 2022
Version of record online: February 16, 2022